

M I S S I N G P A R A M E T E R S I N T H E C M B P H Y S I C S

PAVEL D . N A S E L S K Y

Theoretical Astrophysics Center, Juliane Maries Vej 30, DK -2100,
Copenhagen, Denmark.

Niels Bohr Institute, Blegdamsvej 17, 2100 Copenhagen, Denmark,
Rostov State University, Zorge 5, 344090 Rostov-on-Don, Russia.

A B S T R A C T

The lecture is devoted to the comparison of a few models of cosmic recombination kinetics with recent CMB anisotropy data and to corresponding predictions for the upcoming Planck mission. The influence of additional sources of ionized photons at the epoch of hydrogen recombination may restrict our possibility to estimate the density of baryonic fraction of matter when using Planck data. This new source of degeneracy of the cosmological parameters which can be estimated from the CMB anisotropy data can mimic the distortion of the CMB power spectrum for different models of baryonic matter. I would like to point out that realistic values of the cosmological parameters can not be obtained without Planck polarization data.

1. Introduction

In my lecture, I will discuss the physics of cosmological hydrogen recombination and properties of the last scattering surface (at redshift $z \sim 10^3$), which play a crucial role for the Cosmic Microwave Background (CMB) anisotropy and polarization formation. A detailed understanding of the ionization history of the cosmic plasma is very important in the context of recent CMB experiments, such as the BOOMERANG (de Bernardis et al. 2000), MAXIMA-1 (Hanany et al. 2000), DASI (Halverson et al. 2001), CBI (Mason et al. 2002), VSA (Watson et al. 2002) and especially, the new DASI polarization data (Kovac et al. 2002). I will show how these experiments, including the upcoming MAP and Planck data, would be fundamental for our understanding of the most general properties of the structure and evolution of the Universe, the history of the galaxies and the large-scale structure formation as well. Moreover, the Planck mission will be able to measure the polarization of the CMB with unprecedented accuracy. I will show that polarization power spectra contain all information about the kinetics of hydrogen recombination and allow us to determine the parameters of the last scattering surface and the ionization history of the cosmic plasma at very high redshifts ($z \sim 10^3$).

In the framework of the modern theory of the CMB anisotropy and polarization formation the kinetics of hydrogen recombination are assumed to be "standard" ones. The classical theory of the hydrogen recombination was developed by Peebles (1968), Zel'dovich, Kurlt and Sunyaev (1968) for the pure baryonic cosmological model of the Universe and was generalized by Zlotkin and Naselsky (1982), Jones and Wyse (1985), Seager, Sasselov and Scott (1999), Peebles, Seager and Hu (2000) for non-baryonic dark matter in the Universe. This standard model of recombination has been modified in various ways.

Naselsky (1978) and Naselsky and Polnarev (1987) investigated the evaporation of primordial black holes as a possible source of the hydrogen recombination delay. Avelinet al. (2000), Battye et al. (2001), Landau et al. (2001) have pointed out that possible slow variations in time on the fundamental constants could be important for the ionization history of the cosmic plasma. Sarkar and Cooper (1983), Scott et al. (1991), Ellis et al. (1992), Adams et al. (1998) and Doroshkevich & Naselsky (2002) have investigated the influence of the decays of possible unstable particles on the kinetics of hydrogen recombination and have shown that these particles could be powerful sources for the distortions of the hydrogen ionization fraction. It is worth noting that all the models mentioned above show that the injection of non-thermal high energy electrons and/or photons produces the delay and distortions of the ionization history of the Universe starting from very high redshift $z \sim 10^3$ and down to redshift $z \sim 5 - 10$ when the galaxies started to form. These non-standard models on the ionization history of hydrogen recombination can be characterized by a few additional parameters which we need to take into account in the framework of the best-fit cosmological parameter determination while using recent and future CMB anisotropy and polarization data. I call these parameters as "missing parameters" of the CMB anisotropy and polarization formation theory and I will show how important these parameters are for the CMB physics. The aim of my talk is to compare the possible manifestation of the more complicated ionization history of the Universe with the contemporary CMB anisotropy observational data (BOOMERANG, MAXIMA-1, CBI and VSA) in order to restrict some parameters of the models and to find the best-fit model of the hydrogen recombination, differing from the standard one. I'll show that a set of new parameters related with a more complicated ionization history of the Universe could play a significant role for the upcoming MAP and Planck data.

2. Big Bang and the general properties of the CMB physics

Our knowledge about the Universe is based on the experimental data and the well-developed theory, which we call the Big Bang model: the inflation paradigm, baryogenesis, the theories of cosmological nucleosynthesis of the light chemical element, the formation of the CMB black body spectrum by Compton scattering of photons and electrons, the theories of hydrogen recombination and gravitational instability of the matter in an expanding Universe for the formation of large-scale structure of the Universe. These models serve as a background of the Big Bang theory and play an important role in the modern cosmology. Starting with a very hot and dense phase, the Universe expanded and cooled down. The black body spectra of the

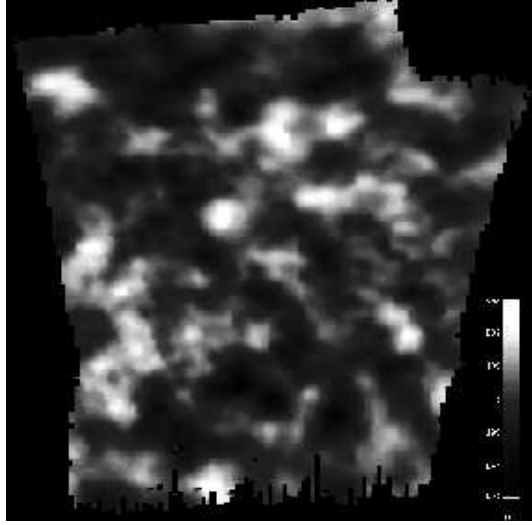


Fig. 1. | The CMB in image of the last scattering surface produced by the MAXIMA-1 experiment.

CMB and, in particular, the angular anisotropy and polarization preserve information about early epochs of cosmological evolution. When the temperature of the cosmic plasma dropped down to $T \approx 3000\text{K}$ the free electrons recombined with protons into neutral hydrogen atoms and primordial hydrogen-helium plasma became transparent to the CMB photons. We call the corresponding redshift $z_r \approx 10^3$ as the redshift of the "last scattering surface", which is the epoch t_r when the Thomson optical depth $\tau \approx 1$. The recombination ceased when the optical depth dropped down to $\tau \approx 0.1$ during the corresponding time interval t_r where $t_r = t_r' \beta = 2 z_r = z_r j \approx 0.1$.

The questions arise as how exactly the cosmological plasma became neutral and how exactly it became transparent to the CMB photons. The answers to these questions lie in the physics of the CMB anisotropy and polarization formation.

The angular anisotropy and polarization of the CMB radiation are related to primordial inhomogeneity of the cosmic plasma just at the epoch of the hydrogen recombination¹. Before this epoch ($z > z_r$) the optical depth of the plasma had been extremely high, so any ripples in the CMB temperature distribution caused by the primordial adiabatic perturbations of the metric, density and velocity of the plasma had been practically erased. After the epoch of recombination the matter component in the Universe became transparent and the CMB photons travel through the space and time from the last scattering surface to the observer. In Fig.1 I show the image of the CMB anisotropy from a small path of the last scattering surface taken by the MAXIMA-1 balloon-borne experiment.

Actually, when we look at the last scattering surface, we see the processes of the structure formation just at the beginning. Small density and velocity perturbations are just traveling compressions and decompression of the photon-electrons gas similar to sound waves. These cosmological sound waves produce the ripples in the CMB map, which corresponds to the hot (white) and cold (black) spots in Fig.1. The cosmological sound waves are quite special. Before recombination the sound speed had been close to $1:7 \cdot 10^6 \text{ km/s}$, but right after recombination it became 3 km/s ! Such drastic transformation of the properties of the matter was described by Andre Sakharov in 1965 in connection with the matter density perturbations. The corresponding prediction by Sakharov is as follows. The amplitude of the perturbations after transition should preserve the modulation from the epoch before the transition should be preserved because of the very high speed of sound

¹ see the lecture notes by A. Lasenby, J. Smoot and A. Melchiorri in this proceeding.

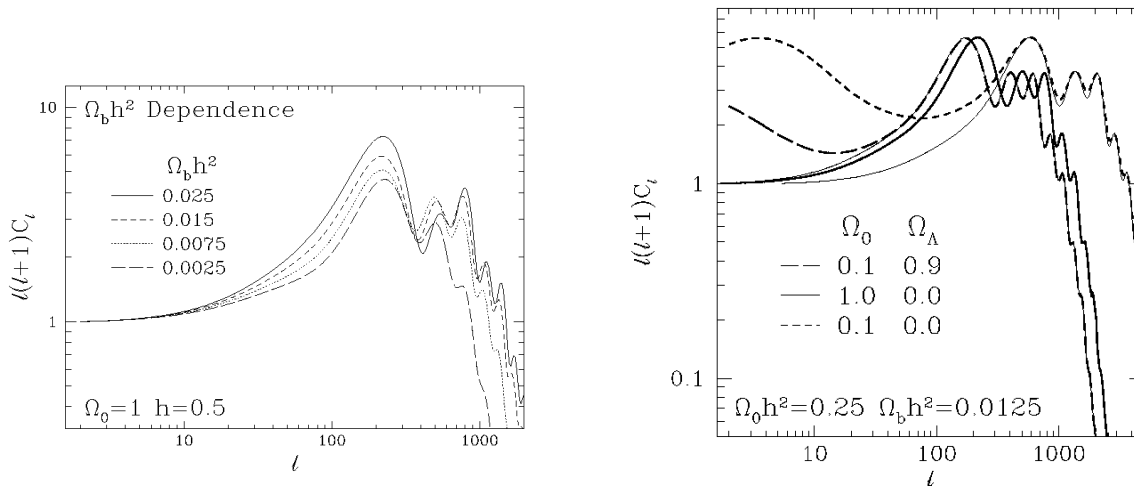


Fig. 2. | The dependence of the CMB power spectrum upon the baryonic and vacuum density parameter, the left and right panel, respectively.

the typical wavelength of the perturbations is close to the size of the horizon at the epoch of recombination. It corresponds to the scale of 300 Mpc at the present moment of the expansion. The ratio between the spatial scale of the fundamental mode, which is 300 Mpc, and the present horizon scale is exactly the angular measure of the CMB anisotropy perturbations, which is close to 30 arcmin.

In discussion which follows, I will use a few characteristics of the CMB anisotropy. Firstly, let me introduce the fluctuations of the temperature T in the spherical coordinate system with polar angle θ and azimuthal angle ϕ .

We can decompose $T(\theta; \phi)$ as a function of θ and ϕ with coefficients $a_{\ell m}$ on a sphere using spherical harmonics $Y_{\ell m}$,

$$T(\theta; \phi) = \sum_{\ell, m} a_{\ell m} Y_{\ell m}(\theta; \phi) \quad (1)$$

The coefficients $a_{\ell m}$ are connected with the amplitudes and the phases of initial metric, density and velocity perturbations, which are the raw material for galaxy formation. This means that the initial conditions of the galaxies formation through the coefficients $a_{\ell m}$ are related to the $T(\theta; \phi)$ distribution in the radio sky.

Using $a_{\ell m}$ we can define the power spectrum of the anisotropy and the perturbation of the temperature $T(\theta)$, which corresponds to the given value of the multipole number ℓ .

$$\langle a_{\ell m} a_{\ell' m'}^* \rangle = C_{\ell} \delta_{\ell \ell'} \delta_{m m'} \quad (2)$$

As one can see from Eq (2), for random Gaussian processes there are no correlations between different harmonics and the phases of the multipoles are uniformly distributed in the range between 0 and 2π .

In Figure 2 I show the numerical calculations of the CMB power spectrum for various cosmological models, which are reproduced from W. Hu's web site². These two panels show the dependence of the CMB power spectrum on the baryonic density parameter $\Omega_b h^2$ and on the vacuum density parameter $\Omega_0 h^2$.

As one can see from Fig 2 (a), the shape of the power spectrum looks like a set of peaks with fixed

²<http://background.uchicago.edu/~whu/>

positions. For a flat universe the first peak corresponds to multipole number $l \approx 200$. The second one $l \approx 400$, the next one $l \approx 600$ and so on.

This is the manifestation of the sound waves in the power spectrum, which was predicted by Sakharov in 1965 and was widely discussed in the literature related to the formation of the CMB anisotropy and polarization power spectrum. In Fig.2 (b) the dependence of the position and the amplitudes of the CMB anisotropy power spectrum peaks have shown for the Λ - and open CDM cosmological models for the given values of baryonic density $\Omega_b h^2 = 0.0125$. As one can see from this Figure, the CMB anisotropy power spectrum reflects directly all peculiarities of the Λ CDM cosmological model related with the geometry of the Universe at the redshifts $z \approx 0.5$.

So, taking the above-mentioned properties into account, we can conclude that all peaks of the CMB anisotropy power spectrum form the basis for a new era of the so-called "precision cosmology". Namely, major attentions of the COBE, BOOMERANG, MAXIMA-1, DASI, VSA, CBI experiments focus on determination of the power spectrum of the CMB anisotropy and testing of the statistical properties of the signals. In addition, all experimental teams have reported on the best-fitting cosmological models, which result in the most probable values of the baryonic matter density Ω_b , the density of the cold dark matter Ω_{cdm} , the density of the vacuum Ω_Λ , possible tilt of the power spectrum of the adiabatic perturbation n_s , the optical depth of reionization τ , the curvature parameter Ω_K and so on, using most probable value of the Hubble constant $h = H_0 / (100 \text{ km sec}^{-1} \text{ Mpc}^{-1}) \approx 0.65 - 0.70$. It is necessary to note that these values of cosmological parameters are obtained from very time-consuming methods, which include as a rule 6 or 11 and more variables such as $\Omega_b; \Omega_c; \Omega_K; n_s; \tau; h$ and so on (e.g. see Tegmark et al. 2001). These parameters describe the most general properties of the Universe starting from very early epoch and down to the present moment of the expansion.

An intriguing question is why we need to use 6, 11 or more parameters for determination for the most realistic cosmological model. The best explanation for high-dimensional space of the cosmological parameters has been suggested by Yu. N. Parijskij. Let us suppose that we have only one peak in the CMB power spectrum, i.e. the first peak at $l \approx 200$ (see Fig.2 a,b). For qualitative description of the peak we need three parameters: the amplitude of the peak, its width and location. For two peaks in the power spectrum, obviously, we need to introduce extra 3 parameters and for three peaks another 3 parameters and so on. From Fig.2 we clearly see that at the multipole range $l \approx 1500$ the number of peaks in the CMB power spectrum is $N = 5$ and thus corresponding number of independent parameters should be 15. So, generally speaking, the space of the cosmological parameters should be high-dimensional because of the peak-like shape of the CMB anisotropy power spectrum.

Let me remind you very briefly of some general properties of the cosmological parameter determination from the CMB anisotropy data sets. The parameter dependence leads to the following definition of the CMB power spectrum for the initial adiabatic perturbations,

$$C_l = C(\Omega_b; \Omega_{dm}; \Omega_c; \Omega_K; n_s; n_t; \tau; r; \dots) \quad (3)$$

where Ω_{dm} is the dark matter density (including cold and warm components) scaled to the critical density of the matter Ω_c , $\Omega_K = 1 - \Omega_b - \Omega_{dm} - \Omega_c$ is the curvature parameter, which determines the flat, close or open model of the Universe, and n_s, n_t are the density of massless and massive neutrino, n_s is the spectral index for adiabatic perturbations (e.g. $n_s = 1$ for the Harrison-Zeldovich power spectrum), n_t is the corresponding spectral index for the gravitational waves, $r = C^t(l=2)/C^s(l=2)$ is the ratio of the gravitational waves and scalar C_l power spectrum at $l=2$, τ is the optical depth of the hydrogen-helium reionization caused by the first quasar and galaxy activity. The notation [i] in Eq (3) is the main topic of my lecture, meaning that some additional parameters resulting from the history of hydrogen recombination could play a significant role in the transition of "the CMB power spectrum! cosmological parameters". Obviously, for the standard model of recombination we assume [i] = 0, which means that we do not need any additional parameters in Eq (3). If the kinetics of hydrogen recombination is distorted, however, by any sources of ionization or have some peculiarities of the spatial distribution of baryonic fraction, then it is necessary to include a few new parameters to the standard scheme. The question is how many parameters can characterize the more

complicated ionization history of hydrogen recombination at redshifts $z \approx 1000 - 1500$? In order to answer this question it is necessary to examine in details the "standard model" of hydrogen recombination.

3. The standard recombination: an approximate model

The recombination of free electrons with protons into neutral hydrogen atoms during the cosmological expansion means that atomic physics, and more specifically, the physics of hydrogen and helium atoms, contain some characteristics of the recombination process, which does not depend on the cosmology and can manifest themselves in a laboratory. Obviously, the corresponding atomic parameters are related with the structure of the electron energy levels in hydrogen atoms.³ Fortunately for the physics of the CMB anisotropy formation, the physics of the electronic transition rates in hydrogen is well known from theoretical as well as experimental point of view. The frequency ν_{nm} of a photon emitted or absorbed in a transition between two levels of energy in hydrogen with principle quantum numbers n, n^0 is given by well-known equation from quantum mechanics

$$E = h\nu = E_n - E_{n^0}; \quad (4)$$

where h is the Planck constant (not the dimensionless Hubble constant!), and $E_n = Ry n^{-2}$, $Ry = e^2/2a_0 = 13.6\text{eV}$, $a_0 = \hbar^2/m e^2$. To liberate a free electron from a neutral hydrogen atom one needs a photon at least the energy $E = h\nu_{n, n^0} = I_n$, where I_n is the ionization potential from the initial state n . For $n = 1$ the corresponding potential is exactly $I = Ry = 13.6\text{eV}$ and I_n decreases as n^{-2} for $n > 1$. But it is exactly what we have in the cosmology just before the hydrogen recombination!

As mentioned in the Introduction, the "hot" Big Bang model of the Universe indicates that the most widespread component in our Universe is the CMB photons, which has a perfect black-body spectrum and the corresponding number density of the photons $n \approx 420\text{cm}^{-3}$ at the present time of the cosmological evolution. In comparison, the number density of baryons $n_b \approx 2 \cdot 10^{-7} (\Omega_b h^2 = 0.02)$ is significantly smaller than the CMB photons. The corresponding photon-baryon ratio $s = n/n_b \approx 2 \cdot 10^8 (\Omega_b h^2 = 0.02)^{-1}$ is an excellent measure how hot the Universe is. Taking into account the temperature $T_0 = 2.728$ from the COBE data for the black-body CMB spectrum (Bennet et al. 1996), we can find the number density of the Ly γ quanta ($I = 10.2\text{eV}$) in the Wien regime of the spectrum $n(E)$ at the present time,

$$n = \int_I^{\infty} n(E) dE \approx n \exp\left(-\frac{h\nu}{kT_0}\right) \quad (5)$$

where $I = h\nu$ is the energy of the Ly γ quanta and k is the Boltzmann constant. If we reverse the cosmological expansion and trace back in time the temperature of the black-body radiation increases and in terms of the redshifts it corresponds to $T(z) = T_0(1+z)$. When the redshift z is close to the redshift of the last scattering surface (z_r), then $T(z_r) \approx 2700\text{K}$ and the corresponding energy $E = kT(z_r) \approx 0.3\text{eV}$. Thus, the number density of the Ly γ quanta at $z = z_r$ is $n(z_r) \approx 2 \cdot 10^{15} n$ and increase rapidly for the higher redshifts and reach the number density of baryons at $z \approx 1500$. For the Ly γ quanta with $E = I = 10.2\text{eV}$ the number density $n_c = n \exp[(I - I_0)/kT(z)] \approx n$ at the redshifts $z \approx 1500$ and decreases rapidly when $z \ll z_r$. So, taking properties of the electron transition in a hydrogen atom into account, one can conclude that photo-ionization of the neutral hydrogen atoms by the Ly γ and Ly γ_c quanta from the CMB power spectra should be a one of the main process of the recombination kinetics.

One additional remark comes from the analysis of the photo-ionization cross-sections for resonant Ly γ and Ly γ_c quanta with neutral hydrogen atoms. In the framework of the theory of the CMB anisotropy and polarization formation the last scattering surface is characterized by the Thomson cross-section $\sigma_T = 8/3 (e^2/mc^2)^2 \approx 6.65 \cdot 10^{-25}\text{cm}^2$, where e and m are the charge and the mass of an electron, and the

³I will discuss the kinetics of hydrogen recombination as a mean process of the formation of the last scattering surface. The kinetics of the cosmological helium recombination is included in the standard RECFAST code (Seager, Sasselov and Scott 1999) and I send the reader to that paper.

corresponding optical depth $\tau_{ph} = \int_{z_r}^z n_{H_i} \sigma_{ph} dt$. For the photo-ionization of neutral hydrogen atoms which forms during the epoch of hydrogen recombination the corresponding optical depth

$$\tau_{ph}(z) = \int_{z_r}^z n_{H_i} \sigma_{ph} dt = \frac{\sigma_{ph}(z)}{c} \int_{z_r}^z n_{H_i} dt \quad (6)$$

where n_{H_i} is the number densities of excited hydrogen atoms at different energy levels of the electrons, $\sigma_{ph}(z)$ is the corresponding cross section of photo-ionization from the excited energy levels of the electrons to the continuum, c is the speed of light and $x_{e,i} = n_e/n_{H_i}$. In the quantum theory of the spectral lines we have the following normalization of the photo-ionization cross sections (see for the reviews by Rybicki and Lightman 1979)

$$\int_0^{\infty} \sigma_{ph}(z) dz = \frac{e^2}{m c} f_{n \rightarrow n^0} \quad (7)$$

where $f_{n \rightarrow n^0} = f_{n,n^0}$ is called the oscillator strength for the transition between states n and n^0 . For example, the Ly transition ($n=1; n^0=2$) in hydrogen yields the $f_{1,2}$ value $f_{1,2} = 0.4162$ (Rybicki and Lightman 1979). Thus, we can conclude that for the Ly transition the corresponding optical depth in the center of the line is approximately more than 10 orders of magnitude higher than the Thomson optical depth at the redshift z_r . For the bound-free transition for hydrogen corresponding cross-section is given by the formula (Rybicki and Lightman, 1979):

$$\sigma_{bf} = \frac{64}{3} \frac{ng}{3} a_0^2 \frac{h\nu}{I_n} \quad (8)$$

where g is the Gaunt factor, $\alpha = e^2/\hbar c = 1/137$ is the fine-structure constant, $a_0 = \hbar^2/m e^2$ and $h\nu = I_n$, $I_n = \frac{1}{2} m c^2 = 2n^2$ is the ionization potential for the $n \rightarrow \infty$ continuum transition. For Ly γ quanta the corresponding cross-section is $\sigma_{bf} \approx 10^{-26} \text{ cm}^2$ and the optical depth is approximately 6 orders of magnitude higher than the Thomson optical depth at the moment of recombination. So, as one can see from the above-mentioned properties of the photo-ionization cross section, the CMB photons play an important role in the kinetics of hydrogen recombination in the Universe. Following Zeldovich, Kurt and Sunuyaev (1968) and Peebles (1968), let us discuss the quantitative model of this process during the epoch $z < 1500$.

3.1. Approximate theory of hydrogen recombination

As it was mentioned above in the expanding Universe the free electrons recombine with protons into neutral hydrogen atoms when the temperature of the matter-photon fluid drops down to $T \approx 3000 - 4000$ K. As the first step of our investigation on the recombination process we have considered the distribution among the levels of a single atom in thermal equilibrium. We want to determine the distribution of an atomic species among its various stages of ionization, which is described by the well-known Saha equation. This equation describes the early stages of hydrogen recombination. Using the so-called three levels of the electron-energy model of hydrogen atom as shown in Fig.3, we can start to describe the transition of the electron from the ground level to the continuum in thermal equilibrium (Rybicki and Lightman 1979).

According to the Boltzmann law the differential number of ions at the ground level ($N^+(v)$) with the free electrons at the velocity range between v and $v + dv$ is

$$\frac{N^+(v)}{N_0} = \frac{g}{g_0} \exp \left(-\frac{I + \frac{1}{2} m v^2}{kT} \right) \quad (9)$$

where N_0 and g_0 are the number and statistical weight of the hydrogen atoms at the ground state, $I = 13.6 \text{ eV}$ is the ionization potential, $g = g_0^+ g_e$ is the product of the statistical weight of the ion at the ground state (g_0^+) and the differential electron statistical weight $g_e = 2d^3x d^3p/h^3$. (Note that the factor 2 in g_e reflects the two spin states of the electron.) The volume element $d^3x = n_e^{-1}$, where n_e is the number density of the free

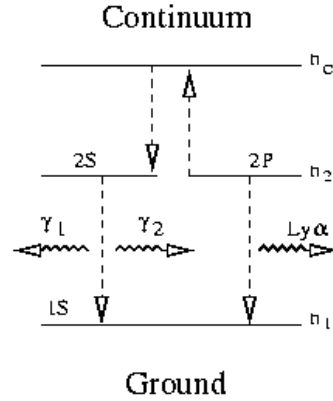


Fig. 3. | The three electron energy levels model of the hydrogen atom .

electrons, and the volume element d^3p is equivalent to $4\pi m^3 v^2 dv$ assuming isotropic velocity distribution. Using Eq. (9) after integration over all v we obtain

$$\frac{n_p n_e}{n_0} = 2 \frac{g_0^+}{g_0} \frac{2\pi m kT}{h^2}^3 \exp(-I/kT) \quad (10)$$

where n_p is the number density of protons and n_0 is the number density of the hydrogen atoms at the ground level. As one can see from Eq. (10) the fraction of free electrons decreases very fast during the cosmological expansion because of the exponential factor $\exp(-I/kT)$. However, I would like to put forward two important remarks while applying the Saha equation for the kinetics of cosmological hydrogen recombination. Firstly, it is necessary to note that during recombination the thermal equilibrium between black-body radiation and atoms has been affected by the deviation of the radiation spectrum from the Planckian form. Since recombination occurs for $kT \sim I$ the number density of photons with $h\nu = I$ would be far smaller than the number density of electrons and protons. The range of the photon spectrum that is crucial for the recombination process actually changes substantially if recombining electrons proceed directly to the ground state. Secondly, it is necessary to take into account the cascading recombination process, which plays the most important role in the recombination kinetics and produce corresponding delay of hydrogen recombination relative to the "standard" fast Saha recombination kinetics. The importance of the cascading recombination process was pointed out by Zeldovich, Kurt and Sunyaev (1968) and Peebles (1968). For the cascading recombination approximation we can neglect the direct recombination to the ground state but introduce the net recombination to the level $(n; l)$,

$$\frac{d}{dt} \frac{n_e}{n_b} = n_{n>1}^{-1} \sum_{n>1} n_{n1} n_e^2 - n_{n1} n_{n1} \quad (11)$$

where n_{n1} is the recombination coefficient to the $(n; l)$ level of energy, n_{n1} is the number density of the excited hydrogen atoms, n_{n1} is the rate of photo-ionization of a hydrogen atom at this level and n_b is the number density of baryons at redshift z . Assuming that the process of recombination does not perturb significantly the black-body spectrum of the CMB at $h\nu = I$ range, the ratio of n_{n1} to n_{n1} is given by the Saha equation for $n \geq 2$,

$$n_{n1} = \sum_{n>1} (2l+1) n_{n1} \exp\left(-\frac{I - I_n}{kT}\right) = n_{n1} \frac{(2\pi m kT)^{3/2}}{h^3} \exp\left(-\frac{I}{kT}\right); \quad (12)$$

where $c = \sum_{n>1} n_{n1}$ and I_n is the potential of ionization from the level n . In addition, it is necessary to take into account that in equilibrium the number density of atoms at the level n satisfies the following

$$n_{n1} = n_{2s} (2l+1) \exp \left[-\frac{I_n}{kT} \right] \quad (13)$$

So, from Eq (11)-(13) we obtain the well-known relation for the number density of the free electrons (Peebles 1968),

$$n_b \frac{d}{dt} \frac{n_e}{n_b} = c n_e^2 - c G n_{1s}; \quad (14)$$

where $G = n_{2s} = n_{1s}$ is the number of photons per mode in the Ly resonance line.

Let me describe briefly the evolution of the resonance Ly line at the epoch of hydrogen recombination (Zeldovich, Kurland and Sunyaev 1968, Peebles 1968). One of the most important results from the Ly photo-ionization cross section is that the mean free time of the resonance recombination line of photons becomes very short, at the order of 30 seconds while the age of the Universe at the redshift $z = 1500$ is at the order of 10^{12} s. That means that the optical depth for the Ly photons at the center of the line is extremely high, at the order of 10^{10} and the radiation in the line is strongly coupled with the formed hydrogen atoms. On the other hand, the cosmological expansion of the Universe redshifted the Ly photons from the center of the line and decrease rapidly the cross section of photo-ionization. To obtain the magnitude of the redshift effect, we can use the approximate equation for the spectrum of the electromagnetic radiation (Peebles 1968),

$$n_b \frac{d}{dt} \frac{n}{n_b} = H(t) (n_{max} - n_{min}) + R(t); \quad (15)$$

where

$$n = \int_{\nu_{min}}^{\nu_{max}} n(\nu) d\nu \quad (16)$$

and $H(t)$ is the Hubble parameter, ν_{min} and ν_{max} are the minimal and maximal frequencies just below and above the center of the line, $n(\nu)$ is the spectral number density of the photons in the line, $R(t)$ is the net rate of production of the Ly photons per unit volume during $2p \rightarrow 1s$ transition. In order of magnitude, taking Eq. (16) into account, we have $n \approx n_{min} \Delta\nu$, where $\Delta\nu$ is the Ly line width and $\nu_{min} \approx 10^5$. Thus, from Eq. (15) one can obtain (Peebles 1968)

$$n_{min} = n_{max} + R H^{-1}(t) \quad (17)$$

Using dimensionless variable $G = c^3 n(\nu) = 8^{-2}$, we can change the last equation to the following form

$$G = G_+ + R H^{-1}(t) = 8; \quad (18)$$

where G_+ corresponds to $n(\nu_{max})$. Because of the intimate contact with the atoms the number of photons per mode satisfies the equation $G_+ = \exp \left[-\frac{I_n}{kT} \right]$ and for G in Eq. (16) we get

$$G = \exp \left[-\frac{I_n}{kT} \right] + R H^{-1}(t); \quad (19)$$

The last point of the approximate model of hydrogen recombination is related to the estimation of the net recombination $R(t)$, which defines the ionization fraction of the hydrogen. Thus

$$R(t) = c n_e^2 - c G n_{1s} = \lambda_{2s;1s} n_{2s} - n_{1s} \exp \left[-\frac{I_n}{kT} \right] \quad (20)$$

where $\lambda_{2s;1s} = 8.227 \text{ sec}^{-1}$ is the decay rate from 2s state. The excess of recombination over photo ionization results in the production of the Ly quanta (the first term in Eq. (20)) or in a two-quantum decay of the

meta-stable 2s level of energy of the hydrogen atom (the last term in Eq. (20)). So, after simple algebra from Eq. (15)-(20) we obtain the well-known equation for the free electron number density (Peebles 1968):

$$n_b \frac{d}{dt} \frac{n_e}{n_b} = C - c n_e^2 - c n_{1s} \exp \left(\frac{I - I_c}{kT} \right); \quad (21)$$

where

$$C = \frac{1 + K_{2s;1s} n_{1s}}{1 + K_{2s;1s} + c n_{1s}}; \quad (22)$$

and $K = \frac{3}{4} H^{-1}(t) = 8$. It is necessary to note that the approximate model of hydrogen recombination assumes that the temperature of the plasma T_m during the recombination process is equivalent to black-body radiation temperature and the contribution of the helium atoms is negligible. A more general and detailed model of recombination was developed by Seager, Sasselov and Scott (1999), which includes the Compton interactions between electrons and photons and the corresponding deviation T_m and T_{cmb} , recombination of helium and ionization by the electrons. The qualitative theory of the hydrogen and helium recombination was summarized in the RECFAST program, which was incorporated in the CMBFAST code (Seljak and Zaldarriaga 1996) for calculations of the power spectrum of the CMB anisotropy and polarization for various cosmological models. Below we will use the modification of the RECFAST and CMBFAST codes to investigate more complicated than "standard" recombination regimes.

4. Delayed and accelerated recombination

As it was mentioned in Introduction and Section 3, the standard model of hydrogen recombination assumes that at the epoch $z \approx 1500$ the production of the resonant Ly α and Ly γ photons is determined by the black-body spectra of the CMB and transitions of electrons into the neutral hydrogen atoms. Generally speaking, any decay of some relics of the cosmological evolution of matter in the Universe at the epoch of recombination are negligible. This assumption, however, needs to be proven by recent and future CMB experiments, especially by the Planck observation.

As it was mentioned in Introduction a lot of non-standard models have been developed during last few years especially for the upcoming Planck experiment, which is characterized by unprecedented accuracy of the anisotropy and polarization power spectrum determination. The aim of this section is to compare the possible manifestation of the more complicated ionization history of the Universe with the contemporary CMB anisotropy observational data (BOOMERANG, MAXIMA-1, CBI and VSA) in order to put constraints on some parameters of the models and to classify the models of hydrogen recombination, differing from the standard one.

The basis for classification of any models of delayed and accelerated recombination is related with the model proposed by Peebles, Seager and Hu (2000), in which two independent parameters μ and μ_i are introduced as effective of the non-thermal resonant Ly α and ionized-photon production before, during and after the period $z' \approx 10^3$,

$$\frac{dn}{dt} = \mu H(t) n_H; \quad (23)$$

and

$$\frac{dn_i}{dt} = \mu_i H(t) n_H; \quad (24)$$

where n_H is the fraction of neutral hydrogen. In their model the parameters μ and μ_i are assumed to be constant in time, which means that corresponding number density of the Ly α and ionized-photon production per interval H^{-1} are $n = H^{-1} dn = dt = \mu n_H$ and $n_i = H^{-1} dn_i = dt = \mu_i n_H$. As one can see, if $\mu \ll 1$ and $\mu_i \ll 1$ then the corresponding distortions of the recombination kinetics should be small. It is natural to assume that the corresponding number density of free electrons produced by photo-ionization of the neutral hydrogen atoms is proportional to n_i and n and corresponds to the electron ionization fraction $x_e = n_{i=n_H} = \mu_i$ or $x_e = n = \mu$ for different stages of hydrogen recombination. However, the

concrete values and possible variation of the Γ and Γ_i parameters in time depends on the energy injection spectra of the sources of the non-thermal resonant Ly γ , ionized photons production and on the model of the source decay.

Let us suppose that all resonant and ionized photons are the result of some massive unstable particles decay (Doroshkevich and Naselsky 2002), which include primordial black hole evaporation. For such particles the number density decreases in time as

$$\frac{dn_X}{dt} + 3H(t)n_X = -\frac{n_X}{\tau_X(n_X; t)}; \quad (25)$$

where n_X is the number density of the X-particles, and $\tau_X(n_X; t)$ is the life time, which can be constant for the standard decay or as a function of cosmological time, if the production of the ionized and resonant quanta is related with annihilation of the X particles. After normalization $n_X = \bar{n}_X \frac{a_0}{a}^3$, where a_0 is the scale factor of the Universe at some moment t_0 , we can transform Eq. (25) to the following form

$$\frac{d\bar{n}_X}{dt} = -\Gamma_X(t)H(t)\bar{n}_X; \quad (26)$$

where

$$\Gamma_X = (\Gamma_X)_0 \exp\left(-\frac{t-t_0}{\tau_X}\right) \frac{\bar{n}_{X, in}}{n_H} \quad (27)$$

and $\bar{n}_{X, in}$ is the initial number density of the X-particles at the moment t_0 .

I would like to point out that Eq. (26) has a general character. Obviously, we can include to the function $\Gamma_X(t)$ all models of the particle decay and then Γ and Γ_i should be proportional to $\Gamma_X(t)$. As the result, they are functions of time (or redshift z).

For illustration of the tight dependency Γ , Γ_i and $\Gamma_X(t)$ parameter, let me describe the model of the Super Heavy Dark Matter (SHDM) particle decay during the cosmological expansion. Such a model was discussed in connection with the origin of the Ultra High Energy Cosmic Rays (UHECRs) in our Galaxy in the framework of so-called Top-Down scenario. As was suggested by Berezhinsky, Karshel'nie and Vilenkin (1997), Kuzmin and Rubakov (1998), Birkel and Sarkar (1998), the formation of such UHECRs can be related to decays of the various kinds of SHDM particles with masses $M_X \sim 10^{12} \text{ G eV}$. This model was widely discussed in connection with AGASA (Hayashida et al. 1994; Ave et al. 2000), Fly's Eye (Yoshida and Dai 1998; Abu-Zayyad et al. 2002)⁴, Haverah Park (Lawrence, Reid and Watson 1991) experiments.

4.1. Expected flux of high energy photons

As is commonly believed, decays of SHDM particles into the high energy protons, photons, electron-positron pairs and neutrinos occurs through the production of quark-antiquark pairs ($q\bar{q}$), which rapidly hadronize, generate two jets and transform the energy into hadrons ($\sim 5\%$) and pions ($\sim 95\%$) (Blaes 1999). It can be expected that later on the energy is transformed mainly to high energy photons and neutrinos. This means that, for such decays of SHDM particles with $10^{12} \text{ G eV} < M_X < 10^{19} \text{ G eV}$, the UHECRs with energy $E > 10^{20} \text{ eV}$ are dominated by photons and neutrinos (Blaes 1999). This conclusion can be tested with further observations of the UHECR fluxes at $E > 10^{20} \text{ eV}$.

Probable energy losses of neutrinos are small (Bhattacharjee and Sigl 2000), they are concentrated at the range $E \sim E_{inj} \sim E_{GZK}$ and could be responsible only for relatively rare observed events. But the comparison of expected and observed fluxes of high energy photons restricts some properties of SHDM particles and the Top-Down model as a whole (Berezhinsky, Blaes and Vilenkin 1998). At high redshifts the interaction of high energy photons with $E \sim E_{inj} \sim E_{GZK}$ with the CMB background ($UHECR + CMB \rightarrow e^+ + e^-$) leads to formation of electromagnetic cascades (Greisen 1966; Zatsepin and Kuzmin 1966).

⁴ see for details E. Loh's lecture in this proceeding

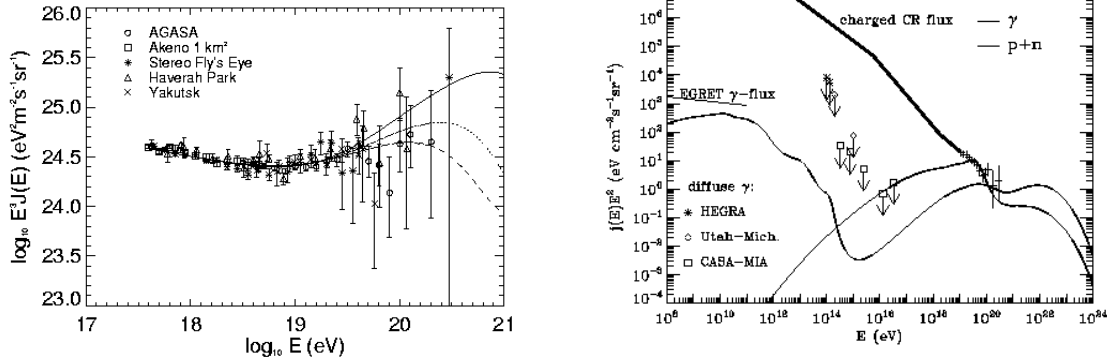


Fig. 4. | The left panel: the observed spectrum for the UHECR and Top-Down scenario predictions for different M_X . The dash line is for $M_X = 10^{11} \text{ GeV}$, the dot line $M_X = 10^{12} \text{ GeV}$, and the solid line $M_X = 10^{13} \text{ GeV}$. (From Sarkar and Toldra 2002. The right panel: the γ -rays spectra from UHECR in comparison with EGRET data. See for details in Sigl (2001).

At small redshifts the efficiency of this interaction decreases and the evolution of such photons depends upon unknown factors such as the extragalactic magnetic field and properties of radio background.

The expected domination of products of decay of the X -particle by the high energy pions and photons follows from quite general arguments. The cumulative contribution of the photons is bigger than the cumulative contribution of the hadrons by a factor of ~ 1.5 . This means that, at least for the galactic component, the cumulative observed flux of UHECRs at energy $E > E_{GZK}$ is also dominated by galactic component of photons with $E > E_{inj} > E_{GZK}$. The discrimination of high energy photon component of UHECRs can be considered as the crucial test for the Top-Down models.

Summarizing available information about the photon component of UHECRs, Bhattacharjee and Sigl (2000) estimate the spectrum of injected photons for a decay of a single X -particle as follows:

$$\frac{dN_{inj}}{dE} = \frac{0.6(2 - \alpha) f}{M_X} \frac{2E}{0.9 M_X} ; E > \frac{M_X}{2} \quad (28)$$

where f is the fraction of the total energy of the jet carried by pions (total pion fraction in terms of number of particles), $0 < \alpha < 2$ is the power index of the injected spectrum, M_X is the mass of the SHDM particles. For the photon path length $l \sim 10 \text{ Mpc}$ at $E > E_{GZK}$ in respect to the electron-positron pair creation on the extragalactic radio background (see Bhattacharjee and Sigl (2000); Protheroe and Biermann 1996) we get for the photon flux $j_{inj}(E)$ at the observed energy E :

$$j_{inj}(E) \approx \frac{1}{4} l(E) n_X \frac{dN_{inj}}{dE} \quad (29)$$

where n_X is the decay rate of the X particles. For the future calculation we will use the normalization of $j_{inj}(E)$ on the observable UHECR flux which corresponds to normalization on the decay rate n_X at present time, $t = t_u$ (Bhattacharjee and Sigl 2000):

$$n_{X,0} \approx 10^{46} \text{ cm}^{-3} \text{ s}^{-1} M_{16}^{-1} x ; \quad (30)$$

where

$$x = \frac{0.5}{2} \left(\frac{0.9}{f} \right) \left(\frac{10 \text{ Mpc}}{l(E_{obs})} \right) (2E_{16})^{3-2} \frac{E_{obs}^2 j_{obs}(E_{obs})}{1 \text{ eV cm}^{-2} \text{ s}^{-1} \text{ sr}^{-1}} \quad (31)$$

and $M_{16} = M_X = 10^{16} \text{ GeV}$, $E_{16} = E_{\text{obs}} = 10^{16} \text{ GeV}$, E_{obs} and $j_{\text{obs}}(E_{\text{obs}})$ are the observable range of the UHECR energy and flux, respectively. Note that normalization (30) does not depend on the nature of the x -particles.

An additional possibility for non-equilibrium high energy photon injection to primordial hydrogen-helium plasma at the epoch of recombination comes from the theory of primordial black hole evaporation (Naselsky 1978; Ivanov, Naselsky and Novikov 1994; Kotok and Naselsky 1998; Doroshkevich and Naselsky 2002) or relatively low massive particle decay $M_X = 10^{12} \text{ GeV}$ (Scott, Rees and Sciamaglia 1991; Adams, Sarkar and Sciamaglia 1998). For primordial black holes with masses $M_{\text{pbh}} = 10^3 \text{ gram}$ the corresponding lifetime is $t_{\text{pbh}} = t_{\text{r}}$ and they evaporate just at the epoch of hydrogen recombination by emitting high energy particles with black body spectra with effective temperature $T_{\text{pbh}} = 10^3 - 10^4 \text{ K}$ and energy $E_{\text{pbh}} = kT_{\text{pbh}} = 1 - 10 \text{ GeV}$ (Hawking 1975). As one can see, this range of energy injection is sufficiently smaller than for the SHDM particles with $M_X = 10^{12} \text{ GeV}$. Note that for the models from Scott, Rees and Sciamaglia (1991) and Adams, Sarkar and Sciamaglia (1998) the characteristic energy of injected photons from neutrino decay is of the order $10 - 100 \text{ eV}$, which is close to the $L_{\gamma} - L_{\gamma}$ energy range. Taking the above-mentioned properties of the non-equilibrium photon injection into account it is natural to expect that practically all range of energy above $L_{\gamma} - L_{\gamma}$ threshold should be very important for investigation of the non-standard recombination kinetics.

4.2. Electromagnetic cascades at the epoch of the hydrogen recombination.

The decays of X -particles cannot significantly distort the thermodynamic of the universe at high redshifts $z = 10^3$ but this injection of energy changes the kinetic of recombination at $z = 10^3$ that leads to observable distortions of the power spectra of CMB anisotropy and polarization. To evaluate these distortions we need firstly to follow the transformation of high energy injected particles to UV photons induced directly the recombination process.

The electromagnetic cascades are initiated by the ultra high energy jets and composed by photons, protons, electron-positrons and neutrino. At high redshifts, the cascades develops very rapidly via interaction with the CMB photons and pair creation ($U_{\text{HECR}} + C_{\text{MB}} \rightarrow e^+ + e^-$), proton-photon pair production ($U_{\text{HECR}} + C_{\text{MB}} \rightarrow p^+ + n^0 + e^+ + e^-$), inverse Compton scattering ($e_{\text{UHECR}} + C_{\text{MB}} \rightarrow e^0 + \gamma^0$), pair creation ($e_{\text{UHECR}} + C_{\text{MB}} \rightarrow e^0 + e^- + e^+ + \gamma^0$), and, for neutrino, electron-positron pair creation through the Z -resonance. As was shown by Berezhinsky et al. (1990) and Protheroe et al. (1995), these processes result in the universal normalized spectrum of a cascade with a primary energy E which can be written as follows:

$$N(E; E_0) = F(E; E_0) \int_{E_c}^E \frac{dE'}{E'} \left(\frac{E'}{E_a} \right)^{\alpha} \left(\frac{E'}{E_c} \right)^{\beta} \left(\frac{E'}{E} \right)^{\gamma} \quad (32)$$

$$F(E; E_0) = \frac{E E_0^2}{2 + \ln(E_c/E_a)} \int_{E_0}^E N dE = E$$

where $E_c = 4.6 \cdot 10(1+z) \text{ GeV}$, $E_a = 1.8 \cdot 10(1+z) \text{ GeV}$. At the period of recombination $z = 10^3$ and for lesser redshifts both energies, E_a and E_c are larger than the limit of the electron-positron pair production $E_{e^+e^-} = 2m_e = 1 \text{ MeV}$ and the spectrum (32) describes both the energy distribution at $E = E_{e^+e^-}$ and the injection of UV photons with $E = E_{e^+e^-}$. However, the spectrum of these UV photons is distorted due to the interaction of photons with the hydrogen-helium plasma.

In the range of less energy of photons, $E = 2m_e$, and at higher redshifts, $z = 10^4$, when equilibrium concentrations of H_{I} , H_{eI} and H_{eII} are small and their influence is negligible, the evolution of the spectrum of ultraviolet photons, $N_{\text{uv}}(E; z)$, occurs due to the injection of new UV photons and their redshift and Compton scattering. It is described by the transport equation (Berezhinsky et al. 1990)

$$\frac{\partial N_{\text{uv}}}{\partial z} + \frac{3N_{\text{uv}}}{1+z} + \frac{\partial}{\partial E} N_{\text{uv}} \frac{dE}{dz} + \frac{Q(E; z)}{(1+z)H} = 0;$$

$$\frac{1}{E} \frac{dE}{dz} = \frac{1}{1+z} + \frac{c_T n_e}{(1+z)H(z)} \frac{E}{m_e c^2} = \frac{1 + (E; z)}{1+z}$$

$$Q(E; t) = n_X N(E; M_X) \quad (33)$$

where the Hubble parameter is

$$H(z) = H_0 \sqrt{\frac{\Omega_m}{1+z} + \Omega_\Lambda} \quad (34)$$

and $n_e / (1+z)^3$ is the number density of electrons, so, $\propto (1+z)^{3-2} E$. Here $Q(E; t)$ is considered as an external source of UV radiation.

The general solution of equation (33) is (Doroshkevich and Naselsky 2002):

$$N_{UV}(z) = \int_{z_m}^z \frac{Q(x) E^2(x)}{H(x) E^2(z)} \frac{1+z}{1+x} \frac{dx}{1+x}; \quad (35)$$

$$E(x) = \frac{1+x}{1+z} E(z) \left(\frac{2}{5} (E; z) \frac{1+x}{1+z} \right)^{5/2} \quad (36)$$

where the maximal redshift, z_m , in (35) is defined by the condition $E(x) = 2m_e c^2$.

As is seen from (35), the Compton scattering dominates for $E \approx 30 \text{ keV}$, when

$$(E; z) = 44 \frac{E}{m_e c^2} \frac{0.3 h_b}{m \cdot 0.02} \frac{1+z}{10^3} \approx 1; \quad (36)$$

$$N_{UV}(z) / \frac{n_X(z) N(E; M_X)}{H(z) (E; z)} / \frac{1+z}{E^{5/2}}(z); \quad (37)$$

For the most interesting energy range, $E \approx 30 \text{ keV}$, $(E; z) \approx 1$, we get again

$$N_{UV}(E(z); z) \approx \frac{2 n_X(z)}{3 H(z)} N(E; M_X = 2); \quad (38)$$

It is necessary to note that the UV photons energy spectra Eq. (38) reflect directly the simple idea that practically all energy of the SHDM relics transforms to the energy of the quanta at the range $E \approx 100 \text{ GeV}$ (at $z = 0$) (see Fig 4b) and then the soft part of the spectra forms due to electromagnetic cascades. At higher redshift, especially at $z \approx 10^3$ the electromagnetic cascades from the γ -range of the spectra are very effective for the UV photon production because of the high energy density of the CMB (12 orders of magnitude higher than the present energy density) and because of increasing of the mean energy of the CMB photons, which is in order of magnitude equivalent to 1 eV .

4.3. Delay of the hydrogen recombination due to SHDM decay

Let me briefly discuss the relationship between initial spectra of the SHDM decay and corresponding parameters η and η_i of the hydrogen excitation and ionization. As it was mentioned in the previous subsection, the spectra of UV photons can be normalized to the energy density of injection $Q(t)$ from the SHDM decay as

$$N(E) \approx \frac{Q}{E_a^2 [2 + \ln(E_c/E_a)]} \frac{E}{E_a} \approx 1; \quad (39)$$

where η is the efficiency of the energy transformation from the $E \approx M_X = 2$ range to the γ range of the photons energy spectra. Let us normalize the energy density of injection $Q(t)$ ($\text{eV cm}^{-3} \text{ s}^{-1}$) to the present day value $Q(t_0)$

$$Q(t) = \eta(t) Q(t_0) \quad (40)$$

where t_U is the age of the Universe at $z = 0$ and $\dot{n}_x(t)$ according to Eq. (25). Integration Eq. (39) over all energies of the photons corresponds to the net of the energy density injection $\dot{n}_x = \int dE \dot{N}_x(E) = \dot{n}_x(t) Q(t_U)$. But for the energy range $E < I$ the net of the ionized UV photons is given by integral $\int dE \dot{N}(E)$:

$$\dot{n}_i = \frac{\dot{n}_x(t) Q(t_U)}{I} \frac{I}{E_a(z)} \frac{1}{2} \quad (41)$$

Using normalization for the energy density $\dot{n}_x H^{-1}$ to the EGRET energy density $\dot{n}_{EGRET} = 410^{-7} \text{eV cm}^{-3}$ (Sigl 2001) of the quanta at the present moment of the cosmological expansion, we can estimate the function $\dot{n}_x(t)$. Namely, assuming

$$\dot{n}_x(t) / t^{4-p} / (1+z)^{\frac{3}{2}(4-p)} \quad (42)$$

we can find that

$$\dot{n}_i = \dot{n}_x(z) \frac{\dot{n}_{EGRET}}{I_{nb}(z=0)} (1+z)^{\frac{3}{2}(1-p)} / (1+z)^{2(1-\frac{3}{4}p)} \quad (43)$$

where $\dot{n}_x(z) = (I=E_a(z))^{1-2} / 3 \cdot 10^{-6} \frac{1}{1+z}$. The power index $p = 1$ correspond the model involving release of x-particles from topological defects, such as ordinary cosmic strings, necklaces and magnetic monopoles (see for review by Sigl 2001). The model $p = 2$ corresponds to the SHDM exponential decay (see Eq. (25)) with $\dot{n}_x = t_U$. From Eq.(43) one can see that for $p = 4/3$ the \dot{n}_i and \dot{n}_x parameters does not depend on the redshift, which is exactly the case of the model by Peebles, Seager and Hu (2000).

One additional possibility comes from the model with $\dot{n}_x = t_U$. This model could be related with primordial black holes evaporation or all SHDM relics decay, for which the corresponding life time is less than the present age of the Universe. Note that for $\dot{n}_x = 0 < t_U$ (and corresponding redshift $z_x = 6-7$) the SHDM relic decay before or just at the galaxy formation epoch and the observable flux of the UHECRs mostly should relate with extragalactic background of the particles, which is characterized by very small anisotropies. For such a model we need to modify Eq. (43) as $\dot{n}_{mod}(z) = \dot{n}_x(z) (z_x/z)$, where

$$\dot{n}_x(z_x) = \exp \left(\frac{h}{kT} \right) (1+z_x)^{\frac{3}{2}p} \quad (44)$$

and z_x corresponds to the \dot{n}_x .

In Fig.5 I show the dependence of the \dot{n}_i parameter on the redshift z for various models of the SHDM decay (for different p and $\dot{n}_x(z_x)$).

As one can see from Fig.5, some of the SHDM relics can distort the kinetics of hydrogen recombination quite significantly ($\dot{n}_i = 10^{-3} - 10^{-2}$ for $z < 1500$), for some of the SHDM relics the perturbation of the ionization history of the Universe is small and practically unobservable. However, all energy injection during the epoch of hydrogen recombination would be partially absorbed by the hydrogen atoms and produce corresponding delay of recombination or ionization of the neutrals.

The question is we can have the acceleration of the hydrogen recombination and what we need to know about the properties of the cosmological plasma beyond the standard model?

4.4. Acceleration of recombination

In the framework of non-standard recombination models, it was shown that all peculiarities of the hydrogen photo-ionization kinetics can be described in terms of \dot{n}_i parameters, which correspond to additional non-equilibrium Ly $_{\alpha}$ and Ly $_{\gamma}$ photon injection. In the previous section it was shown that for different models of the SHDM particles decay both parameters \dot{n}_i are positive and hence the delay of hydrogen recombination occurs. In terms of the \dot{n}_i parameters any acceleration of recombination means that one or both of them are negative. However, any decay of the SHDM relics do not produce "negative" energy injection and, taking into account the black-body CMB photons, acceleration of the recombination means that we can remove

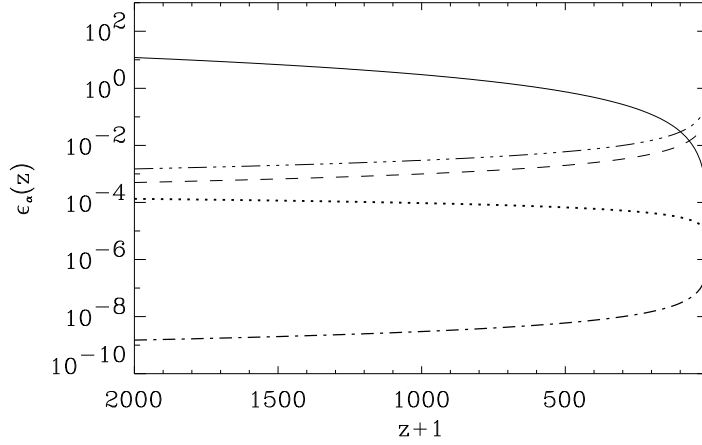


Fig. 5. The dependence of the ϵ_s parameters versus z for different models of the SHDM decay. Solid line corresponds to $p = 0$; $(z_X) = 1$ model, dot line is $p = 1$; $(z_X) = 1$ model, dash-dot line is the model $p = 2$; $(z_X) = 1$ and dash line and dash-dabble dot line are the models $p = 2$; $(z_X) = 10^6$ and $p = 2$; $(z_X) = 3 \cdot 10^6$ correspondingly.

some of the photons from interaction with the formed neutral hydrogen atoms, which is impossible. Does it mean that for given values of the cosmological parameters (Ω_b ; Ω_m ...etc.), which determine the general properties of the model of the Universe, we can only have the delay of hydrogen recombination? To answer this question, we need to focus on Eq. (21), in which the net of free electron number density decreases during recombination which is proportional to the electron and proton number density. The non-linear dependence of the ionization fraction on baryonic number density is the key to the construction of the accelerated model of recombination!

The basic idea of accelerated recombination is very transparent (Naselsky and Novikov 2002). Suppose that, instead of pure adiabatic model of initial metric, density and velocity perturbation of matter we have the mix between adiabatic and isocurvature (or isothermperature) perturbation. If at the very small mass scales of isocurvature perturbations, e.g. those comparable with $10^2 - 10^5 M_\odot$, the distribution of the baryons is very non-uniform like clouds, beyond which scale perturbations follow the standard adiabatic properties, then the hydrogen recombination inside the clouds goes faster than outside the clouds. This indicates that for adiabatic perturbations which produce anisotropies and polarization of the CMB, the hydrogen ionization differs from the standard one, which corresponds to the mean value of the baryonic matter density. Non-trivial is that such a modification of the ionization history of the hydrogen in the cloudy baryonic model can be described in terms of $\epsilon_s < 0$ and $\epsilon_s > 0$ parameters as for the delayed recombination model (Naselsky and Novikov 2002). All of these delayed and accelerated recombination models could be very important for reconstruction of the best-fitting cosmological model parameters from the modern CMB observational data and can distort the optimal values.

5. Non-standard recombination and its manifestation in the CMB anisotropy and polarization power spectrum

For illustration of the introduced above classification of the hydrogen recombination regimes we will use two cosmological models with the following parameters. The Model 1: $\Omega_b h^2 = 0.022$; $\Omega_c = 0.125$; $\Omega_k = 0$; $\Omega_s = 0.7$; $r = 0.1$; $h = 0.7$; $n_s = 1$; $\epsilon_s = \epsilon_i = 0$. This model has the best-fitting of the CBI observational

data (Mason et al 2002). The Model 2: $\Omega_b h^2 = 0.032$; $\Omega_c = 0.115$; $\Omega_K = 0$; $\tau = 0.7$; $r = 0.1$; $h = 0.7$; $n_s = 1$; $\alpha = \alpha_i = 0$. This model differs from the previous one on the baryonic and CDM fraction densities and it is non-optimal according to the CBI data. Using RECFAST code we can find the differences in the ionization fraction of hydrogen plotted in Fig. 6.

Fig.7 is the plot of the ionization fraction of the hydrogen in the clumpy baryonic model (Model 3), which corresponds to the parameters of the Model 1, but instead of $\Omega_b h^2 = 0.022$ we have to use the mean value of the baryon density $\Omega_b h^2 = 0.022$, assuming that density contrast between inner and outer regions $\rho_{in} = \rho_{out} = 11$, the fraction of volume in clouds $f = 0.1$ and the mass fraction $Z = f/[1 + (1-f)] = 0.5$.

The mass spectrum of a clouds means to be close to $(M - M_{cl})$, where $10^2 M < M_{cl} < 10^6 M$. For this model the mean ionization fraction is related with ionization fractions inside x_{in} and outside x_{out} clouds as $x_{mean} = x_{in} Z + x_{out}(1 - Z)$ (Naselsky and Novikov 2002). In Fig.8 we show the difference between x_{mean} and x_1 normalized to $(x_1 + x_{mean})/2$.

As one can see from Fig.8, at the range $700 < z < 1500$ we have acceleration of recombination while at the range $z < 700$ we have delay of recombination. The last model, Model 4, which we would like to include in our analysis is the Model 2 plus additional sources of delay and ionization, corresponding to the following values of the α ; α_i parameters:

$$\alpha(x) = \exp \left[\frac{1+z}{1+z_x} \right]^{\frac{3}{2}} \left[\frac{1+z}{1+z_x} \right]^{\frac{3}{2}} ;$$

$$\alpha_i(z) = -\alpha(z) \quad (45)$$

where $\alpha' < 0.3$, $\alpha_i' < 0.04$ and $z_x < 10^3$. As one can see from Eq(6) at $z < 10^3$ the variation of the α ; α_i -parameters are very slow and $\alpha' < \alpha_i'$ for comparison with the parameters by Peebles, Seager and Hu (2000). In Fig.9 I plot the ionization fraction in Model 4 in comparison with ionization fraction in the Model 1 and the Model 2. As one can see the delay of recombination in the Model 4 produce 20-30% deviation of the ionization fraction at the redshift $z < 10^3$ and very significant deviations at the redshift $z < 10^3$.

It is worth noting that all the Models 1-4 clearly illustrate the different delayed and accelerated regimes, discussed at the beginning of the this section. The question is how sensitive the CMB anisotropy and polarization power spectrum on different models of ionization history of hydrogen and baryonic density? Below I will show that combination Ω_b ; α ; α_i is very important for estimation of the correct value of the baryonic fraction density from the CMB data.

5.1. Anisotropy and polarization as a test on ionization regimes

In order to compare the CMB anisotropy and polarization power spectrum in the Models 1-4 we have to use modification of the CMBFAST code (Seljak and Zaldarriaga 1996), by taking into account more complicated ionization history of the plasma. All the models which include the late reionization correspond to the standard CMBFAST option for a given value of the optical depth τ . This value of τ is related with the ionization fraction $x = 1$ at the redshift of reionization z_r as

$$z_{re} = 13.6 \frac{\tau}{0.1} \frac{1}{0.76} \frac{Y_p}{0.022} \frac{h^2}{0.125} \quad (46)$$

where Y_p is the helium mass fraction of the matter. In Fig.10 we plot the CMB power spectrum for the Models 1-4 in comparison with the BOOMERANG, MAXIMA-1, and CBI data at the multipole range $l < 2000$ in which the possible manifestation of the Sunyaev-Zeldovich effect is not important.

As one can see from Fig.10 all the models look very similar to each other. However, in the Table 1 we show the values of the τ -parameter for all the models. From the Table 1 we see that the Model 3 with baryonic

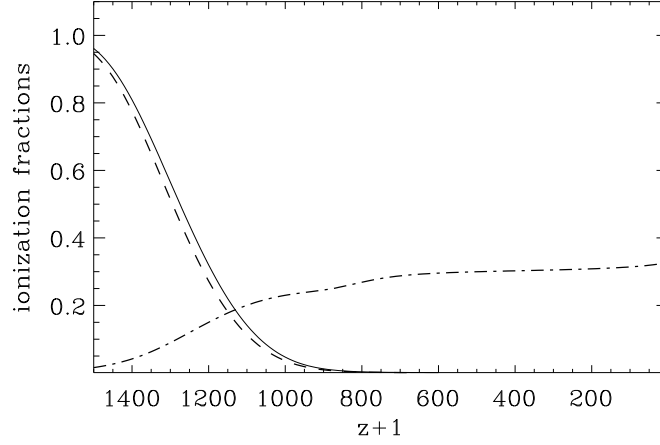


Fig. 6. | The rate of ionization for the Model 1 and 2. Solid line corresponds to the Model 1 (x_1), dash line Model 2 (x_2), dash-dot line the ratio $(x_1 - x_2)/x_1$. The reionization epoch are not included.

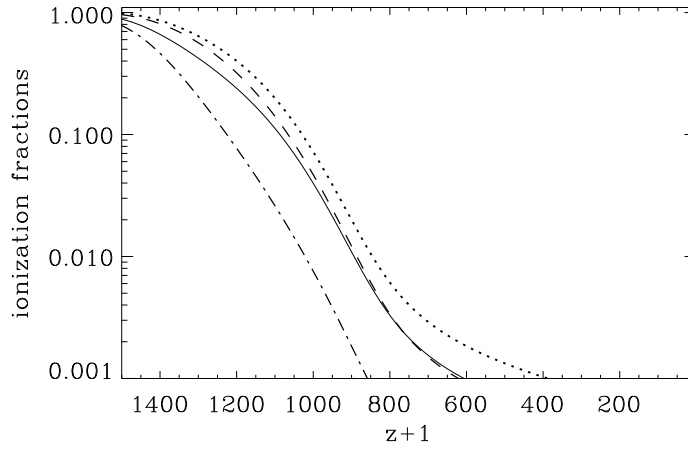


Fig. 7. | The rate of ionization for the clumpy baryonic model. Dash-dot line corresponds to the ionization fraction for the inner regions at. Dotted line is the ionization fraction for the outer regions. Solid line the mean fraction of the ionization. Dash line is the ionization fraction for the model with $\beta_b = 0.045$.

Table 1: χ^2 for observations and models

obs/model	BOOM	MAXIMA	CBIM 1	CBIM 2	VSA
Model 1	11.2	14.1	3.20	7.15	7.08
Model 2	34.6	17.7	2.75	7.51	13.0
Model 3	8.69	11.3	1.60	5.62	6.59
Model 4	27.7	15.7	1.87	5.15	10.0

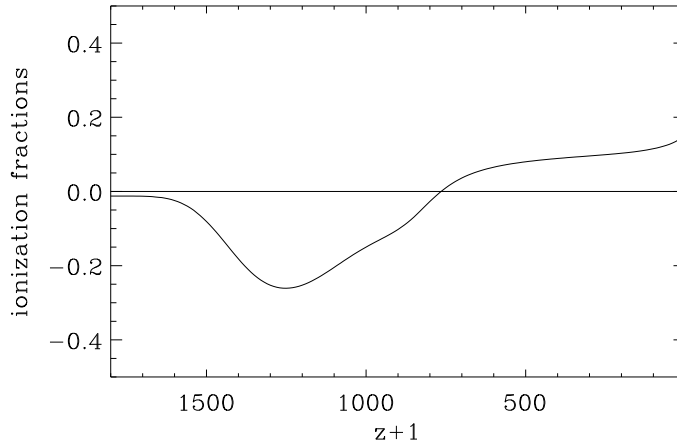


Fig. 8. | The difference of the rates of ionization between the clumpy baryonic cosmological model and without clumps.

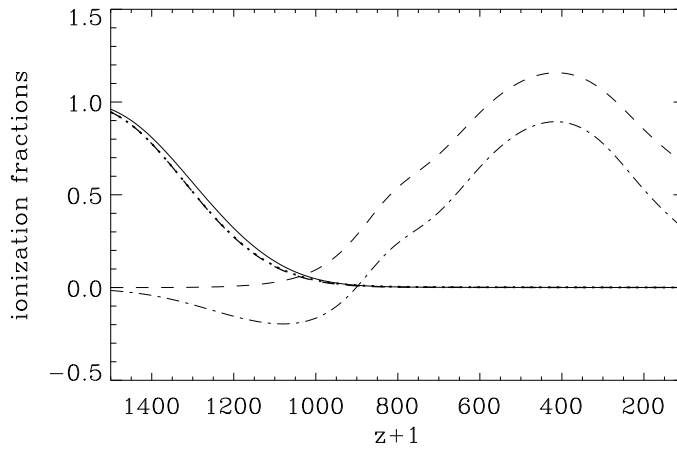


Fig. 9. | The rates of ionization and the differences of the rates of ionization between the Model 1, 2 and 4. Solid line is the ionization fraction in the Model 1. Dotted and short-dash line are the Model 2 and 4, respectively, which look very similar. Long-dash line corresponds to the ratio $2(x_4 - x_1)/(x_1 + x_4)$. Dash-dot line corresponds to $2(x_4 - x_2)/(x_2 + x_4)$.

clouds has an excellent agreement with the CBI data while the Model 1 is characterized by the value of the $\frac{\sigma_1^2}{\sigma_2^2} = 2 \frac{\sigma_1^2}{\sigma_2^2}$. Note that the Model 1 is the best-fitting model for the CBI data without any assumption on more complicated ionization history of cosmological hydrogen recombination. The Model 4 corresponds to the σ_1^2 parameter 1.5 times bigger than the Model 1. However, this model also has an excellent agreement with all the CBI observational data.

From the practical point of view, the Models 1, 3 and 4 consistent with the CBI data and more complicated ionization history of the hydrogen recombination manifest themselves as new sources of degeneracy of the cosmological parameters, namely, the baryonic density of matter. This conclusion is very important for the upcoming MAP and Planck data. In order to characterize the differences between the models and to compare their with the sensitivity of the upcoming Planck experiment we plot in Fig. 11 the functions

$$\begin{aligned} D_{1;3}(\ell) &= 2 [C_1(\ell) - C_3(\ell)] = [C_1(\ell) + C_3(\ell)]; \\ D_{2;4}(\ell) &= 2 [C_2(\ell) - C_4(\ell)] = [C_2(\ell) + C_4(\ell)]; \end{aligned} \quad (47)$$

for the multipole range $2 < \ell < 2500$. Obviously, these functions $D_{1;3}(\ell)$ and $D_{2;4}(\ell)$ is necessary to compare with the errors of the C_ℓ extraction for the Planck mission.

As one can see from Fig. 11, the range of the $D_{1;3}(\ell)$ and $D_{2;4}(\ell)$ values is close to the 5%. Note that it can easily drop down to 1-2% using smaller values of the parameters of the non-standard ionization history $\tau; \tau_1$ and corresponding parameters σ, Z, σ, m and so on. These parameters play a role of the "missing parameters" in the model of the CMB anisotropy formation and significantly increase the number of the standard parameters $\sigma_b, \dots, \sigma_k$. It is well known that for analysis of the degeneracy of some of the cosmological parameters the polarization measurements are very useful. In Fig. 7 we plot the polarization power spectrum $T_p^2(\ell) = \ell(\ell+1)2 C_p(\ell)$ for the Models 1-4. As one can see from this Figure, the difference of the $T_p^2(\ell)$ is very small at the range $\ell > 200$ and quite significant for the Model 1 and 2 relatively the Models 3 and 4 because of the bump at $\ell \approx 5-10$, which is related with reionization of the hydrogen at the epoch of formation of galaxies and clusters of galaxies. Some useful information can be obtained at the range $20 < \ell < 200$ in which the manifestation of the Model 4 is significant. This Model shows that the optical depth $\tau = 0.1$ can be obtained without distortions of the low multipole part of the power spectrum at $\ell \approx 5-10$. However, for the Planck mission one of the most important source of uncertainties at the multipole range $\ell < 200$ is the cosmic variance. The corresponding errors of the $T_p^2(\ell)$ estimation at this range is $C_p(\ell) = C_p(\ell) \cdot (f_{\text{sky}})^{1=2} \cdot 9 (\ell=200)^{1=2} (f_{\text{sky}}=0.65)^{1=2} \%$.⁵ For $f_{\text{sky}}=0.65 \cdot 1$ and $\ell > 2000$ the cosmic variance limit on $C(\ell) = C(\ell)$ is 3% at 68% confidence level, which means that all the peculiarities of the anisotropy power spectra below this limit should be unobservable. For the CMB polarization, as it follows from Fig. 8 all features of the power spectrum can be observed by the Planck and probably, the low multipole part of the power spectrum can be observed by the MAP mission. So future experiments for detection of polarization can be very useful for investigation of the ionization history of the cosmic plasma and possible distortions of the kinetics of hydrogen recombination by the different sources.

6. Conclusion

The precision of the measurements on the CMB anisotropy and polarization, especially being expected from the MAP and Planck missions, allows us to distinguish the cosmological models under consideration and to discuss 10-20% distortions of the standard recombination process occurring at redshift $z \sim 10^3$.

In my talk I have compared available data from observations of the CMB anisotropies with several cosmological models with different kinetics of hydrogen recombination, which is caused by possible external sources of the energy injection and possible small-scale clustering of the baryonic component in the clouds. It was shown that such a sources can produce the delay or acceleration of hydrogen recombination and increases the number of parameters used to fit observed power spectra of the CMB anisotropy and polarization.

⁵We assume that instrumental noise and systematics should be close to the cosmic variance limit.

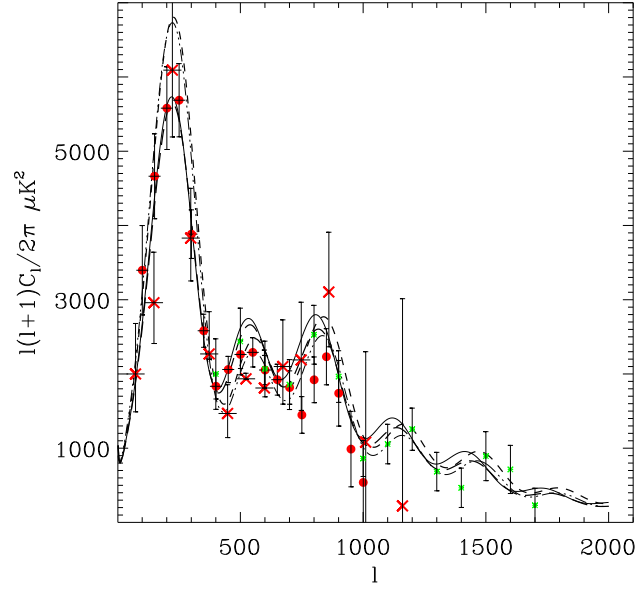


Fig. 10. | The CMB power spectrum for the Models 1-4. Solid line corresponds to the Model 1, dash line the Model 2, dash-dot line the Model 3, and long-dash line the Model 4.

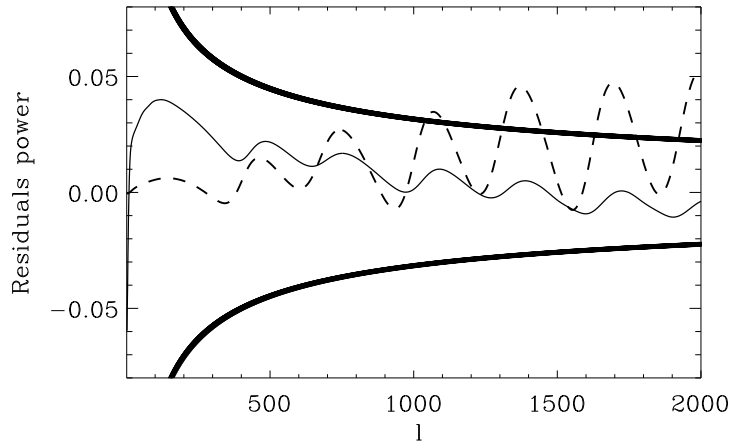


Fig. 11. | The differences in the CMB power spectrum for the Models 1-4. Solid line corresponds to the $D_{1,3}$ (") function and dash line $D_{2,4}$ ("). Thick solid line is the estimated errors for the Planck .

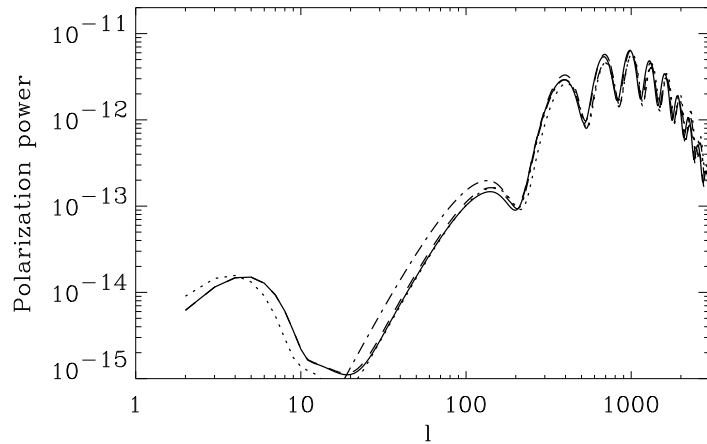


Fig. 12. The CMB polarization power spectrum for the Models 1-4. Solid line corresponds to the Model 1, dot line the Model 2, dash line the Model 3, and dash-dot line the Model 4.

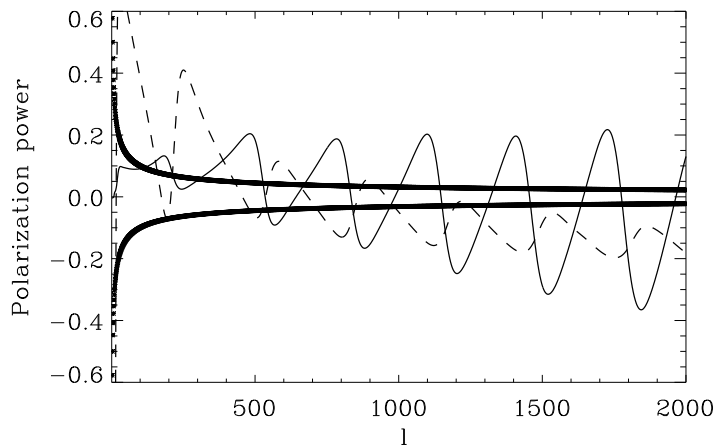


Fig. 13. The differences of the CMB polarization power spectrum for the Models 1-3 and the Models 2-4. Definition for residuals are similar to the definition for the anisotropy. Solid line is for $D_{1;3}$ ($^{\circ}$) and dash line $D_{2;4}$ ($^{\circ}$), but for polarization. Thick solid line is the estimated errors for the Planck .

The most interesting conclusion coming from the investigation of the non-standard models of hydrogen recombination is that the CMB polarization measurements will play an important role for the estimation of the "missing parameters" from the upcoming Planck data.

Acknowledgment

I would like to thank Prof. Norma Sanchez for the invitation to participate this School. This paper was supported in part by Danmarks Grundforskningsfond through its support for the establishment of the Theoretical Astrophysics Center, and by grants RFBR 17625.

I am grateful to L.-Y. Chiang, A. Doroshkevich, I. Novikov and A. A. Starobinsky for discussions and help during the preparation of this article.

7. References

- Abu-Zayyad et al., 2001, *ApJ*, 557, 686
 Adams, J.A., Sarkar, S. & Sciamanda W., 1998, *MNRAS*, 301, 210
 Ave, M., et al., *Phys. Rev. Lett.*, 85, 2244, 2000;
 Avellino, P., Martins, C., Rocha, G., & Viana, P., 2000, *Phys. Rev. D*, 62, 123508
 Battye, R., Crittenden, R., & Weller, J., 2001, *Phys. Rev. D*, 63, 043505
 Bhattacharjee P. & Sigl, G. 2000, *Phys. Rept.*, 327, 109
 Berezhinsky, V. S., Bulanov, S. V., Dogel, V. A., Ginzburg, V. L. and V. S. Pustkin, *Astrophysics of Cosmic Rays*, (North Holland, Amsterdam, 1990)
 Berezhinsky, V. S., Kashelrie, M. & Avilenkin, 1997, *Phys. Rev. Lett*, 79, 4302,
 Berezhinsky, V. S., Blasi, P. and Avilenkin, 1998, *Phys. Rev. D*, 58, 103515
 Birkel M. and Sarkar, S. 1998, *Astropart. Phys.*, 9, 297
 de Bernardis, P., et al., 2000, *Nature*, 404, 955
 Blasi, P., 1999, *Phys. Rev. D*, 60, 023514, .
 Doroshkevich A. G., & Naselsky, P. D., 2002, *Phys. Rev. D*, 65, 123517
 Doroshkevich A. G., Naselsky, I. P., Naselsky, P. D. & Novikov, I. D., 2002, *astro-ph/0208114*
 Ellis, J., Gelmini, G., Lopez, J., Nanopoulos, D., & Sarkar, S., 1992, *Nucl. Phys. B*, 373, 399
 Halverson, N. W., 2002, *ApJ*, 568, 38
 Hayashida, N., et al., 1994, *Phys. Rev. Lett*, 73, 3491.
 Hanany, S., et al., 2000, *ApJ*, 545, L5
 Greisen, K. 1966, *Phys. Rev. Lett.*, 16, 748.
 Jones, B. J. T., & Wæ R., 1985, *A & A*, 149, 144
 Yoshida, S. & H. Dai, 1998., *J. Phys. G*, 24, 905.
 Ivanov, P. B., Naselsky, P. D. and Novikov, I. D., 1994, *Phys. Rev. D*, 50, 7173.
 Kotok, E. V. and Naselsky, P. D., 1998, *Phys. Rev. D*, 58, 103517.
 Kovac, J., et al., 2002, *astro-ph 0209478*.
 Kuzmin, V. A., & V. A. Rubakov, 1998, *Yadern. Fiz.*, 61, 1122
 Landau, S., Harari, D., & Zaldarriaga, M., 2001, *Phys. Rev. D*, 63, 3505
 Lawrence, M. A., Reid, R. J. O. & Watson, A. A., 1991, *J. Phys. G*, *Nucl. Part. Phys.*, 17, 733
 Mason, B. S., et al., 2002, *astro-ph/0205384*
 Naselsky, P. D., 1978, *Sov. Astron. Lett.*, 344, 4
 Naselsky, P. D., & Polnarev, A. G., 1987, *Sov. Astron. Lett.*, 13, 67
 Naselsky, P. D., & Novikov, I. D., 2002, *MNRAS*, 334, 137
 Peebles, P., 1968, *ApJ*, 153, 1
 Peebles, P., Seager, S., & Hu, W., 2000, *ApJ*, 539, L1
 Protheroe, R. J., & Biermann, P. L., 1996, *Astrop. Physics*, 6, 45
 Protheroe, R. J., Stanev, T., and V. S. Berezhinsky, 1995, *astro-ph/9409004*
 Rybicki, G. B. and Lightman, A. P., 1979, *Radiative processes in astrophysics*, A Wiley-Interscience publi-

cation

- Sarkar, S., and Toldra, R., 2002, Nucl. Phys., B 621, 495
Sarkar, S., & Cooper, a., 1983, Phys. Lett. B, 148, 347
Scott, D., Rees, M. J., & Sciama, D. W., 1991, A & A, 250, 295
Seager, S., Sasselov, D., & Scott, D., 1999, ApJ, 523, L1
Seljak, U., & Zaldarriaga, M., 1996, ApJ, 469, 437
Sigl, G., 2001, hep-ph/0109202
Tegmark, M., 2001, A & A S, 199, 3407
Zabotin, N. A., & Naselsky, P. D., 1982, Sov. Astron., 26, 272
Zatsepin G. T., and Kuzm in, V. A., 1966, Pis'm a Zh. Eksp. Theor. Fiz., 4, 114,; JETP. Lett., 4, 78, 1966.
Zeldovich, Ya. B., Kurt, V., & Sunuyaev, R. A., 1968, Zh. Eksp. Theor. Phys., 55, 278
Watson, R. A., et al., 2002, astro-ph/0205378